의학박사 학위논문

The Impact of Zymosan-induced Acute Inflammation on Progression and Metastasis in Pancreatic Cancer Animal Model

실험 동물 모델에서 자이모산을 이용한 급성 염증이 췌장암의 성장과 전이에 미치는 영향에 대한 연구

2016년 2월

서울대학교 대학원

의학과 외과학 전공

안 근 수

의학박사 학위논문

The Impact of Zymosan-induced Acute Inflammation on Progression and Metastasis in Pancreatic Cancer Animal Model

실험 동물 모델에서 자이모산을 이용한 급성 염증이 췌장암의 성장과 전이에 미치는 영향에 대한 연구

2016년 2월

서울대학교 대학원

의학과 외과학 전공

안 근 수

실험 동물 모델에서 자이모산을 이용한 급성 염증이 췌장암의 성장과 전이에 미치는 영향에 대한 연구

지도교수 한 호 성

이 논문을 외과학 의학박사 학위논문으로 제출함

2015년 10월

서울대학교 대학원

의학과 외과학 전공

안 근 수

안근수의 의학박사 학위논문을 인준함

2016년 1월

위 원 장		(인)
부위원장		(인)
위 원		(인)
위 원		(인)
위 원		(인)

Abstract

The Impact of Zymosan-induced Acute Inflammation on Progression and Metastasis in Pancreatic Cancer Animal Model

Keun Soo Ahn

Medicine (Surgery)

The Graduate School

Seoul National University

Introduction Although clinically, acute inflammation is thought to influence the growth of cancer, there have been no preclinical studies on the relationship between acute inflammation and cancer progression. The aim of this study was to evaluate the impact of acute inflammation on cancer progression in an animal model concerning morphological change as well as molecular features reflecting the epithelial-to-mesencymal transition (EMT) and circulating tumor cells (CTC).

Method and materials Murine pancreas ductal adenocarcinoma cell line (Panc-02)

and zymosan were used for the induction of cancer and acute inflammation respectively, in C57/BL6 mice. In the control group (n=10, C group), $2x10^7$ Panc02 cells were injected into the tail of the pancreas and the mice were sacrificed after 4 weeks. In the second group (n=10, Z1 group), Panc02 cell injection was performed and 1 week later, 3mg of zymosan was injected intraperitoneally. The mice were sacrificed 4 weeks after tumor cell injection. In the third group (n=10, Z2 group), after Panc02 cell injection, intraperitoneal injection of zymosan was performed at 1 and 2 weeks after tumor injection respectively, and the mice were sacrificed 4 weeks after tumor cell injection. Histopathological analysis of tumor progression and inflammatory cell infiltration in the three groups was done. Expressions of EpCAM,muc1, E-Cadherin, Snail1, NLRP3 and miR-155 in the tissues were analyzed by confocal microscopy. Additionally, expression of E-Cadherin, Snail1 and Vimentin in the liver tissues were analyzed by reverse transcription polymerase chain reaction (RT-PCR) and western blot.

Results Among the 30experimental mice, seven were excluded four died before autopsy and three displayed no tumors. Autopsies were performed in the remaining 23 mice. Histopathological analysis showed that the tumor volume of the Z2 group was larger than that of the C group (P=0.021) and the presence of liver metastasis was significantly more common in the Z2 group than in the C and Z1 groups

(P=0.025). The degree of inflammation was also more severe in the Z2 group than in the other two groups. Confocal microscopy analysis revealed significantly more expression of EpCAM, muc1,NLRP3 and miR-155 in the liver and pancreas in the Z2 group than in the other two groups. EpCAM and muc1 was detected in blood samples in the Z2group by confocal microscopy and flow cytometry, but not in the other two groups. On RT-PCR and western blot analysis, expression of Snail1 and Vimentin1 in the Z2 group were stronger in the liver compared to the C group. On the contrary, E-Cadherin expression in the Z2 group was weaker compared to the C group.

Conclusion Our results showed that acute inflammation accompanied with cancer promotes cancer progression.

Key words : Acute inflammation, Cancer, Epithelial-to-mesenchymal transition, Circulating tumor cell

Student Number : 2011-31125

Contents

Abstract ---------- i

Contents ----------iv

List of Tables & Figures ---------- v

List of Tables ----------v

List of Figures----------vi

I.Introduction---------- 1

II.Materials and Methods---------- 4

III.Results---------- 14

IV.Discussion---------- 28

V.References---------- 37

Abstract - Korean---------- 46

Acknowledgement---------- 48

List of Tables

Table 1. Histopathologic finding among the three groups

---------- 17

Table 2. Tumor volume and frequency of liver metastasis according to the degree of inflammation

---------- 18

Table 3. The expression of markers by confocal microscopic analysis in pancreas

---------- 19

Table 4. The expression of markers by confocal microscopic analysis in liver

---------- 20

List of Figures

Figure 1. Study design

---------- 13

Figure 2. Gross and microscopic finding in 3 groups (H&E, X200).

---------- 21

Figure 3. Confocal microscopic analysis for NLRP3 and miR-155 in the tissues.

---------- 22

Figure 4. Confocal microscopic analysis for muc1 and EpCAM in the tissues.

---------- 23

Figure 5. Muc1 and Ep-CAM expression in the mice blood.

---------- 24

Figure 6. Confocal microscopy tissue analysis of E-Cadherin and snail 1.

---------- 25

Figure 7. Evaluation E-cadherin, Vimentin and Snail1expression as EMT markers in the liver tissue by qRT-PCR.

---------- 26

Figure 8. Evaluation E-cadherin, Vimentin and Snail1expression as EMT markers in the liver tissue by western blot analysis.

---------- 27

Introduction

The relationship between inflammation and cancer was first suggested by Virchow in the 19th century.[1] He suggested that chronic inflammation mediated by chemicals irritates tissue and that this damage induces the development of cancer. This hypothesis has been proven by several recent studies. Chronic inflammatory disease, such as inflammatory bowel disease, chronic hepatitis, intrahepatic bile duct stone, sclerosing cholangitis and chronic pancreatitis, are risk factors of malignancy.[1-3]Inflammatory cells and cytokines found in tumors may likely contribute to tumor growth, progression and immunosuppression.[4]Cytokines including interleukin (IL)-1, IL-6, tumor necrosis factor-alpha (TNF-α), and cyclooxygenase-2 and prostaglandin secreted by inflammatory cells may activate oncogenes and transcription factors.[5]

However, in contrast to chronic inflammation, there is lack of evidence concerning the relationship between cancer and acute inflammation.[3]Acute inflammation coexisting with cancer frequently produced an adverse effect in the clinical setting and seems to cause poor survival after surgical resection.[6-8] Postoperative inflammation is associated with poor long-term survival in periampullary cancer[9, 10] and colorectal cancer[11], suggesting a specific role of acute inflammation on cancer

progression. However, there is no robust evidence that acute inflammation has a consistent effect on the prognosis of cancer.

Epithelial-to-mesenchymal transition (EMT) is a multi-step process involving molecular and cellular changes in epithelial cells. Normal epithelial cells are cuboidal and remain in contact with other cells through adherent and tight junctions, which are composed mainly of E-Cadherin, Catenins and Actin. They are also attached to the basal membrane by integrins. When restrained and immobile epithelial cells gain a mesenchymal phenotype, characterized by loss of their epithelial junctions, which enhances their motility and the ability to degrade extracellular matrix (ECM); the result is allowed stationary to gain the ability to migrate and invade. This process of EMT is critical in promoting metastasis in epithelium-derived carcinoma.[12, 13] Inflammatory cytokines in the tumor microenvironment can promote EMT.[14, 15] Meanwhile, circulating tumor cells (CTCs) are considered a precursor for metastatic transformation and a predictive factor of tumor relapse.[16]Accumulating evidence indicates that a subset of CTCs and circulating stem cells (CSCs) have an EMT phenotype[17, 18].These EMT-linked CTCs and CSCs enable these cells to survive in the peripheral circulation and actively cause relapse of the tumor. EMT contributes to the intravasation of CTCs from the primary tumor site, followed by transport to a secondary site where the cells extravasate, proliferate and form a metastatic lesion.[19]

Therefore, acute inflammation may influence tumor progression by facilitating the EMT/MET process and CTC intravasation.

Although many studies have assessed the impact of chronic inflammation on cancer, the preclinical and molecular backgrounds of acute inflammation on cancer progression is unclear. The aim of this study was to evaluate the impact of acute inflammation on cancer progression in an experimental mouse model by evaluating the morphological change as well as molecular features reflecting the EMT and CTC.

Materials and Methods

Materials and Reagents

Antibodies to epithelial cadherin (E-cadherin), Snail(both from Santa Cruz Biotechnology,Santa Cruz, CA, USA) and NACHT, LRP and PYD domains-containing protein 3 (NLRP3; ProSci Inc.,Poway, CA, USA) were prepared for confocal microscopy analysis. Immunochemistry reagents were obtained from molecular probe (Invitrogen, Carlsbad, CA, USA). Aptamers(epithelial cell adhesion molecule [EpCAM] and mucin 1, cell surface associated [muc1]) and beacon (miR-155) were synthesized by Bioneer (Daejeon, Korea). Zymosan used for the induction of acute inflammation was from Sigma-Aldrich (St.Louis,MO, USA).

Animal maintenance

Eight-week-old, female, specific-pathogen-free C57/BL/6J mice with body weights of 20-22g were obtained from Oriental Bio (Seongnam, Korea). They were maintained in plastic cages with sterilized paper bedding in a clean and air-conditioned room at 22±2 C°. They were allowed to adapt to the new surrounding for 7 days with free access to a standard laboratory diet and water. All procedures performed on the mice were in accordance with the guidelines of the Animal Care

and Use Committee of Bundang Hospital of Seoul National University, Korea. This study was approved by the Seoul National University Bundang Hospital Institutional Animal Care and Use Committee (BA1109-091/064-01).

Cell culture

Panc02 murine pancreatic ductal adenocarcinoma cell line was obtained from American Type Culture Collection (Rockville, Md, USA). Cells were cultured in Dulbecco's modified Eagle's medium containing 10% fetal bovine serum (FBS; Invitrogen), 10 U/ml penicillin (Invitrogen), and 10 μg/ml streptomycin in a 5% CO_2-humidified chamber at 37°C. Culture cells in multi-well plate chamber slides were incubated overnight or for 2 days until attaining 50 80% confluence. After reaching up to 90% confluency, the medium was aspirated and the cells were washed with phosphate-buffered saline (1xPBS). After trypsin-EDTA treatment, the detached cells were collected in standard culture medium, centrifuged at 1,000 rpm for 5 min and transferred to 100 mm culture dishes.

Cell viability assay

For assessment of Panc02 cell viability before injection into mice, viable adherent cells were stained with 2 mg/ml 3-(4,5-dimethylthiazol- 2-yl)-2,3-diphenyl

tetrazolium bromide (MTT) for 2 h. The medium was removed and the formazan crystals that had formed were dissolved by adding 200 μl dimethylsulfoxide (DMSO). Absorbance was assayed at 570 nm. Cell viability was expressed as the ratio of the treated population versus untreated control cells.

.

Orthotopic implantation of tumor and induction of inflammation

The mice were divided into 4 groups of 10 animals each (Figure 1).In the control group (n=10, C group), mice were sacrificed 4 weeks after tumor cell injection into the pancreatic tail. In the second group (n=10, Z1 group), 2 weeks after tumor injection, a suspension of3mg of zymosan in PBS was injected intraperitoneally, then the mice were sacrificed at 4 weeks after tumor injection. In the third group (n=10, Z2 group), intraperitoneal injection of zymosan was repeated at the 2^{nd} and 3^{rd} weeks after tumor injection, and the mice were sacrificed at 4 weeks after tumor injection. In the normal group (n=10, N group), the mice received no injection of cancer cells or zymosan.

The procedure for pancreatic cancer cell injection in the C,Z1 and Z2 groups are as following. General anesthesia was induced using 2% isoflurane (Ifran, Hana Pharm Com., LTD, Korea) in oxygen and maintained at 1.5% after induction. The abdominal cavity of the mice was opened vertically by a length of vertically. Suspended $2x10^7$

Panc02 cells in 100ul of phosphate-buffered saline (PBS) were directly injected into the pancreatic tail with a pre-cooled calibrated special syringe (Hamilton Syringe, Reno, Nev, USA). Then abdominal cavity was then closed.

Animals were sacrificed by cervical dislocation in deep CO_2 anesthesia. In every mice, 1ml of blood was obtained from heart puncture. Then, the organs including the pancreas, spleen, liver, lung and kidney were harvested and investigated by hematoxylin/eosin (H/E) staining and immunocytochemistry analysis. Tumor volume was measured using follow formula: largest diameter X (smallest diameter)^2 X 0.5.[20, 21]The differentiation of the tumor and the presence of metastasis were analyzed by pathologist. The degree of inflammation was measured by the identification of inflammatory cell infiltration in surrounding pancreatic tissue.

Preparation of fluorescent EpCAM and muc1 aptamer probe

Intelligent NH2/aptamer/COOH nanoparticles (NP) probe (2pmol/mL), 5' - NH2-modified oligos, Ep-CAM (5' - GGGACACAATGGACGTCCGTAGTTCTGGCTGA CTGG TTACCCGGTCGTACAGCTCTAACGGCCG ACATGAGAG-3'), muc1 muc1 (5' - AACCGCCCAAATCCCTAAGAGTCGCAGTTGATCCTTTGGATACC CTGGCACAGA-3') and mutant (mt) (5' - AACCGCCCAAATCCCTTACCCTGG CACAGA-3') were obtained from Bioneer. The methods used to generate a

nanoparticle-based CTC probe using aptamers have previously been reported and are well characterized. [22, 23] Briefly, carboxyl moieties of cy5 or FAM were covalently conjugated to the amino groups of EpCAM or muc1 with the coupling reagent, N-(3-dimethylaminopropyl)-N' -ethyl-carbodiimide hydrochloride) (EDC; Sigma-Aldrich) at an NH2-aptamer. COOH NP probes were prepared with a molar ratio of 1: 1 for 1 h at room temperature. The molar ratio of fluorescent probe for the smart circulating tumor cell probe (EpCAM:NP and muc1 :NP) was each 1:1. Probe conjugates were collected using centrifugal filtration at 15,000 rpm for 30 min and resuspended in Tris-buffer (pH 7.4). The conjugation efficiency between the carboxyl group of the probe and amine group of EpCAM or muc1 was determined by collecting each unconjugated probe in the supernatant after centrifugal filtration of the fluorescence probe conjugate and measuring the concentration using a NanoDrop ND-1000 Spectrometer (NanoDropTechnologies, Wilmington, DE, USA).

Confocal microscopy analysis

Confocal microscopy analysis was done usinga LSM710 laser scanning microscope (Carl Zeiss, Inc., Weimer, Germany) using the following parameters: H33342 imaging; 405/488 nm, FAM-muc1; 488 525 nm, cy5-Ep-CAM: 565 635 nm, E-Cadherin-QD525, Snail1-QD565, NLRP3-QD525 and miR-155 molecular beacon

(QD565- GGCCGGCTCTCCTACCTGTTAGlCATTAACGGGGTTCCTGGGGATGGG

ATTTGCTTCCTGTC ACAAATCACATTGCCAGGGATTTCCAACCGACC-BHQ2).

Tissues from the sacrificed mice were seeded onto 35-mm sterile confocal dishes. After 24 h, tissues were incubated with FAM-muc1and/or cy5-EpCAM. Each mutant was subjected to further labeling procedures for 30 min at 4° C. To remove the unbound conjugates, the cells were washed three times for 10 min each time by shaking incubation (30 rpm) in Tris buffer. Cells were then fixed with 200㎕ of4% formaldehyde solution (Sigma-Aldrich), followed by washing three times with PBS for 10 min each with shaking incubation (20 rpm). Cell nuclei were stained with H33342 solution (Molecular Probes, Eugene, OR, USA) to obtain direct information about the targeting of cy5 conjugated with EP-CAM and muc1 aptamers in the cells and nuclei using high-resolution optical images. The fixed cells were mounted on a slide and the coverslip was placed above 1 ml of H33342 solution. Optical images were obtained at low magnification (100x) and expanded to 200x.

Flow cytometery

EpCAM and muc1 expression in blood was analyzed by flow cytometry using FACScan (BD Biosciences, Piscataway, NJ, USA). The cell density of blood was adjusted to 1×10^5/ml. Two tubes were prepared.Muc1-FAM (2 pmol/ml) and Ep-

CAM-cy5.5 (2 pmol/ml) were added to the separate tubes. The cells were cultured at 37°C in a 5% CO2 culture box for 90 min, rotated and mixed every 15 min and washed twice (5 min each time) with pre-cooled PBS. The cells were resuspended in 400 μl PBS and used for flow cytometry.

Reverse transcription polymerase chain reaction (qRT-PCR)

To determine the levels of mRNA expression, mRNA was extracted from liver tissues using Trizol RNA reagent (Invitrogen). Total RNA was reverse-transcribed in a final volume of 20 μl containing 1 μl of oligo (deoxythymidine), 4 μl of 5_first-strand buffer, 2 μl of 0.1 mol/l dithiothreitol, 1 μl of 10 mmol/L deoxynucleotide triphosphate mix and 50 units of Moloney murine leukemia virus reverse transcriptase (Invitrogen). cDNA was synthesized from 400 ng of the mRNA using a first-strand cDNA synthesis kit (Doctor Protein, Korea). PCR was performed using the following primers: E-cadherin (250bp) 5' primer, 5'-gccccgaaaatgaaaagggcgaa-3' and 3' primer, 5'- taaactctggcctgttgtcat-3'; Snail1 (310bp) 5' primer, 5'-ggatgtgaagagataccagtgc-3' and 3' primer, 5'- aaaggccaccaagagagcca-3; Vimentin (230bp) 5' primer, 5'- ccccaccctgaacctaaacttt-3' and 3' primer, 5'-ggaaaagacaatcactgccc-3'. PCR was performed using the same PCR machine (Takara, Shiga, Japan) in 25 μl of reaction mixture comprising 1 μlcDNA. The reaction

conditions were as follows: 2-min cycle at 94° C, 30 cycles comprising 45 s at 92° C, 45 s at 55° C and 1 min at 72° C, followed by a 5 min cycle at 72° C. PCR products were separated on a 1% agarose gel containing ethidium bromide.

Western blot

Whole cell proteins were prepared according to the instructions of the ProteoJET Cytoplasmic Kit (Thermo Fisher, Pittsburgh, PA,USA). Extracted proteins were quantified by a BCA protein assay. For the analysis of total protein levels of E-Cadherin, Snail1 and Vimentin, stimulated cells were rinsed twice with ice-cold PBS and then lysed in ice-cold lysis buffer (50 mMTris-HCl, pH 7.4), containing 150 mMNaCl, 1% Nonidet P-40, 0.1% SDS, 0.1% deoxycholate, 5 mM sodium fluoride, 1 mM sodium orthovanadate, 1 mM 4-nitrophenyl phosphate, 10 μg/ml leupeptin, 10 μg/ml pepstatin A and 1 mM 4-(2-aminoethyl)benzenesulfonyl fluoride). Cell lysates were centrifuged at 15,000 rpm for 20 min at 4° C, and the supernatant was mixed with a one-fourth volume of 4× SDS sample buffer and boiled for 5 min. Proteins were separated by 10% SDS-PAGE. After electrophoresis, proteins were transferred to a polyvinylidene fluoride membrane using a Trans-Blot SD semidry transfer cell (Bio-Rad, Hercules, CA, USA). The membrane was blocked in 5% skim milk for 1 h, rinsed and incubated with primary antibody in Tris buffered saline Tween

(TBST) and 3% skim milk overnight at 4° C. Excess primary antibody was removed by washing the membrane four times in TBST, and the membrane was incubated with 0.1 μg/ml peroxidase-labeled rabbit secondary antibody for 1 h. Following three washes in TBST, bands were visualized by enhanced chemiluminescence (ECL) Western blotting detection reagents and exposed to x-ray film. Each experiment was repeated independently three times.

Statistical analysis

Continuous variables are reported as means ± standard deviation (SD). Kruskal-Wallis analysis was used to determine if there was a difference in the continuous variables among the groups. The categoric variables were compared using Pearson Chi-square analysis. All the analyses were carried out using SPSS for Windows version 18.0 (SPSS, Chicago, IL, USA). P-values< 0.05 were considered significant.

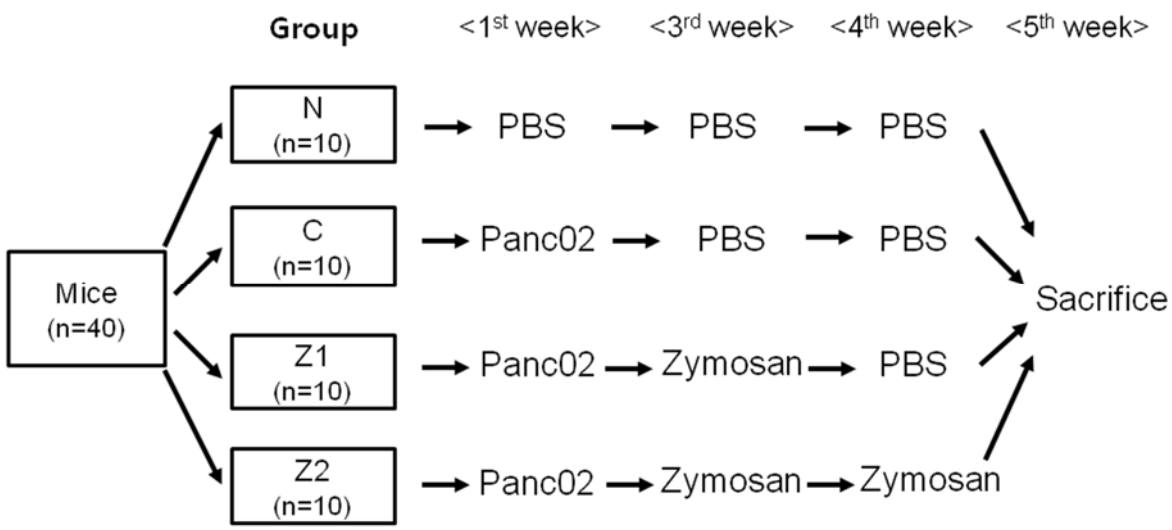

Figure 1. Study design

Results

Histopathological analysis

Among the 30 experimental mice except N group, four died before autopsy: one in the C group, one in the Z1 group and two in the Z2 group. All of them died during week 3 after tumor injection. Causes of death remained unknown. Three mice (one in C group and two in Z1 group) with no tumor formation were also excluded. Finally, autopsy and histopathologic analysis were performed in 23 mice (eight in C group, seven in Z1 group and eight inZ2 group). In all groups, changes of body weight were not significantly different. In the Z2 group, estimated pancreatic tumor volume per body weight was significantly larger than that of the C group (P=0.021).The presence of liver metastasis was significantly more frequent in the Z2 group than in the C and Z1 groups (P=0.025). The degree of inflammation was similar between the C and Z1 groups, but was more significantly severe in the Z2 group compared to the other two groups (Table 1, Figure 2).

In any group, mice with moderate inflammation had a significantly larger tumor volume and more frequent liver metastasis than mice with no inflammation (Table 2).

Expression of markers in the tissues and blood

The expression and intensity of EpCAM, muc1,NLRP-3,miRNA-155, E-Cadherin and Snail1in the pancreas and the liver tissues were performed with confocal microscopic analysis (Table 3 and 4). Additionally, the expression of EpCAM and muc1 were analyzed by confocal microscopy and flow cytometry.

Expression of NLRP3 and miR-155 in the liver and pancreas tissues

Confocal miscoscopy revealed increased colocalization of NLRP3 in the Z2 group, suggesting the formation of NLRP3 inflammasomes in pancreas and liver tissues (Figures 3A and C). Similarly, expression of miR-155 was increased in the Z1 and Z2 groups, but rarely in the N and C groups (Figures 3B and D).

Expression of Muc1 and EpCAM in the tissues and blood sample

Muc1 and EpCAM were prominently expressed in pancreas and liver tissues in the Z2 group, but were weakly expressed in the Z1 group and rarely expressed in the N and C groups (Figure 4).

Additionally, confocal microscopy analysis for detection of muc1/EpCAM expression was independently performed using three 10 μg samples of blood from each mouse. Staining of muc1 and EpCAM were not apparent in the N and C groups. However, in three mice in the Z1 group (42.9%) and all mice in the Z2 group, larger

CTC-like cells that expressed muc1 and EpCAM expression were observed (Figure 5A). Flow cytometry revealed fewer than 0.05% cells positive for muc1/EpCAM cells in the N and C groups, while increased expression of muc1 (1.24%) and EpCAM (5.56%) were evident in the Z2 group(Figure 5B).

Expression of E-Cadherin , snail1 and Vimentin

In the pancreas and liver tissues, prominent expression of Snail was observed in the Z1 and Z2 groups, with rarely expression in the N and C groups (Figures 6). In both tissues, E-Cadherin was expressed strongly in the N, C and Z2 groups, while weakly in the Z1 group(Figure 6).

On the RT-PCR (Figure 7) and Western blot (Figure 8) of the liver tissue, the expression levels of Snail1 and Vimentin were increased in the Z1 and Z2, while rare expression was seen in the N and C groups. On the contrary, E-Cadherin was expressed strongly in the N and C groups, but not in the Z1 and Z2 groups.

Table 1.Histopathologic finding among the three groups

Group	**C (n=10)**	**Z1 (n=10)**	**Z2 (n=10)**	***P****	***P*** †
Death before sacrifice	1	1	2		
No tumor formation	1	2	0		
Body weight (gm, mean ± S.D)	21.4±0.7	21.7±1.1	21.7±0.8	*0.702*[1]	*0.529*[3]
Estimated tumor volume (mm3)	52.2±45.7	103.6± 77.3	147.3±82.1	*0.224*[1]	*0.059*[3]
Estimated tumor volume per body weight (mm3)	2.04±2.13	4.6±3.2	6.7±4.1	*0.057*[2]	*0.021*[3]
Liver metastasis (n,%)	1 (12.5%)	0 (0%)	4 (50.0%)	*0.025*[2]	*0.282*[2]
Inflammation(no/mild/moderate)	6/2/0	4/2/1	0/3/5	*0.025*[2]	*0.015*[2]

C; control group, Z1 :Zymosan once treated group, Z2 : Zymosan twice treated group

*Comparison among the three groups.

† Comparison between C and Z-2 groups.

1 :Kruskal-Wallis analysis.

2. Pearson Chi-square analysis.

3. Mann-Whitney U analysis (between C and Z2 groups)

Table 2.Tumor volume and frequency of liver metastasis according to the degree of inflammation

Group	No inflammation (n = 10)	Mild inflammation (n = 7)	Moderate inflammation (n = 6)	*P*
Number per group (C,Z1,Z2)	6/4/0	2/2/3	0/1/5	*0.015*[1]
Estimated tumor volume(mm3)	69.0 ± 79.4	113.9 ± 55.8	149.2 ± 99.5	*0.030*[2]
Liver metastasis (n,%)	0	2 (28.6%)	3 (50.0%)	*0.013*[1]

1. Pearson Chi-square analysis
2. Kruskal-Wallis analysis.

Table 3. The expression of markers by confocal microscopic analysis in pancreas

	N (n=10)	**C (n=8)**	**Z1 (n=7)**	**Z2 (n=8)**	***P***
Ep-Cam (-/+/++)	10/0/0	8/0/0	5/1/1	1/2/5	<0.001
muc1 (-/+/++)	10/0/0	7/0/1	5/2/0	0/2/6	0.008
NLRP-3 (-/+/++)	10/0/0	8/0/0	4/1/2	0/2/6	0.012
miRNA-155 (-/+/++)	10/0/0	8/0/0	5/1/1/	0/2/6	0.020

Table 4. The expression of markers by confocal microscopic analysis in liver

	N (n=10)	**C (n=8)**	**Z1 (n=7)**	**Z2 (n=8)**	***P***
Ep-Cam (-/+/++)	10/0/0	8/0/0	7/0/0	0/0/8	<0.001
muc1 (-/+/++)	10/0/0	7/0/1	5/2/0	0/0/8	<0.001
NLRP-3 (-/+/++)	10/0/0	8/0/0	4/1/2	2/1/5	0.008
miRNA-155 (-/+/++)	10/0/0	8/0/0	5/1/1/	3/2/3	0.038

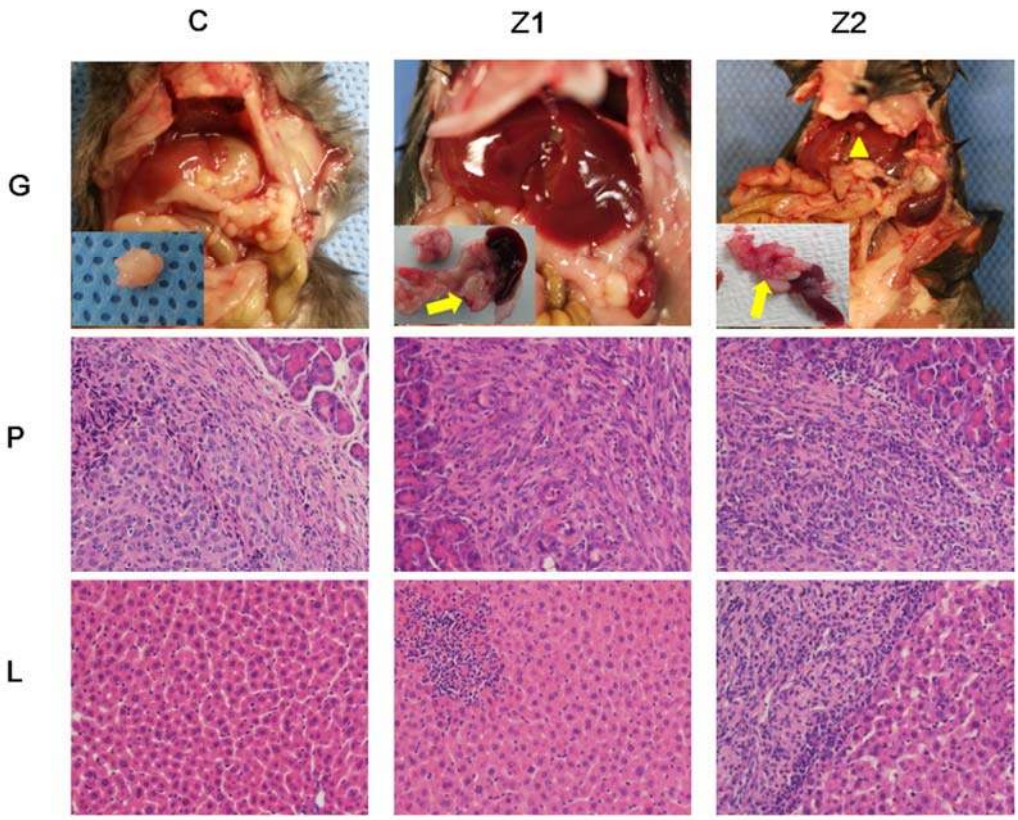

Figure 2. Gross and microscopic finding in 3 groups (H&E, X200). G;1st row: Gross finding, P;2ndrow: Pancreas, L; and 3rd row:Liver. In the control group (column C),round tumor was formed at the pancreas tail (row G). Microscopically, tumor cells displayed marked pleomorphism and bizarre nuclei in the pancreas (row P; left area), but liver tissue was unremarkable. In the Z-1 group (column Z-1), round tumor was noted at the pancreas tail (row G; arrow). In pancreas tissue, infiltration of tumor cells and a few inflammatory cells were evident (row P; right area). In liver tissue, a few inflammatory cells were evident (row L; left upper area), with no tumor cells visible. In the Z-2 group (columnZ-2), irregular pancreatic tail tumor (arrow) and metastatic nodule on the liver surface (arrow head) were seen in gross appearance (row G). Tumor cells were admixed with inflammatory cells in pancreas tissue (row P ; right area) and liver tissue (row L; left area).

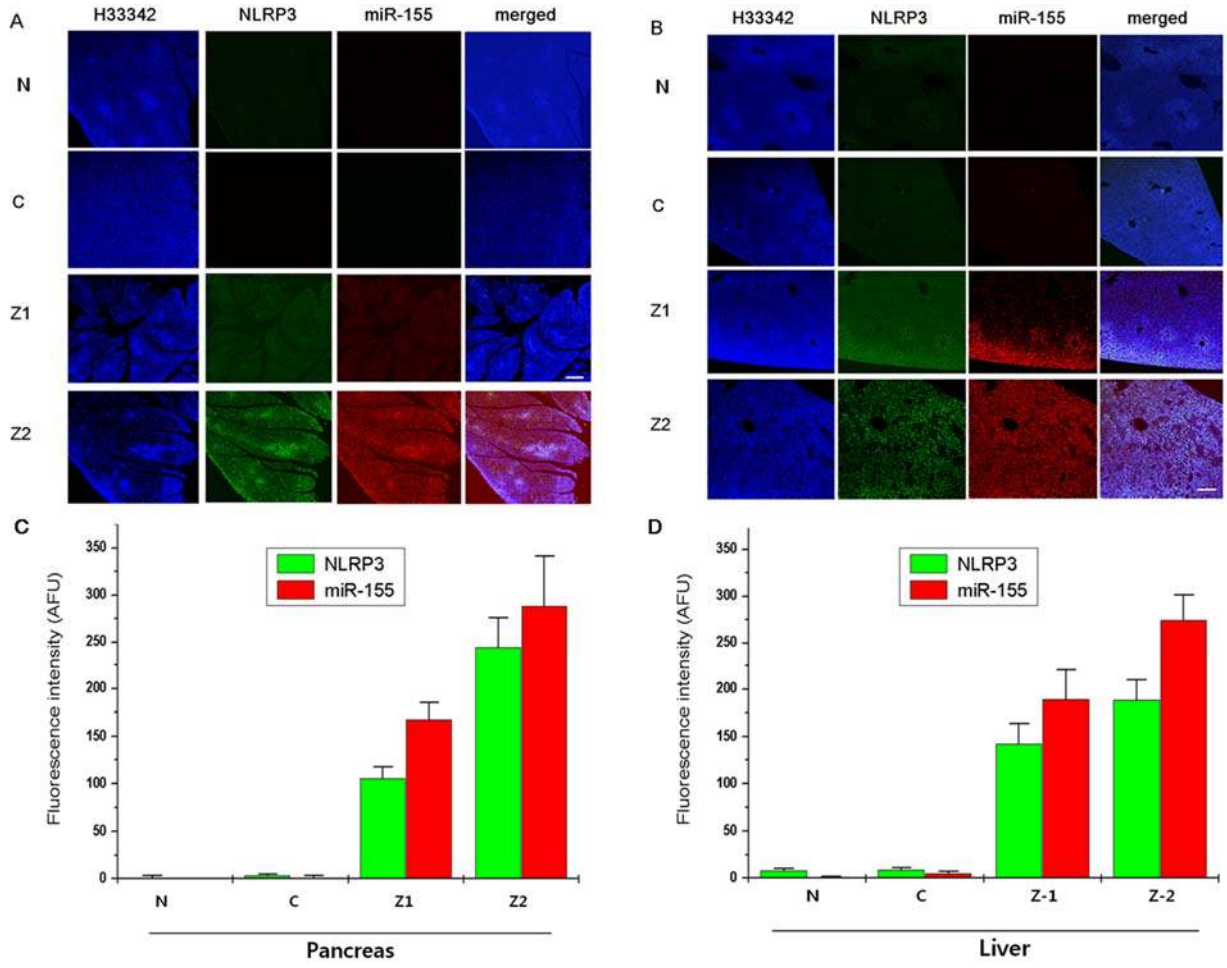

Figure 3.Confocal microscopic analysis for NLRP3 and miR-155 in the tissues.

Tissues were immunocytochemicaly stained to detect NLRP3 (green) and miR-155(red) with H33342 (blue) to mark nuclei. Scale Bars denote 55 μm. In the pancreas (A and C), expression of both markers are gradually increased in the Z1 and Z2, but these markers are rarely expressed in the N and C. Similar patterns are observed in the liver tissues (B and D).

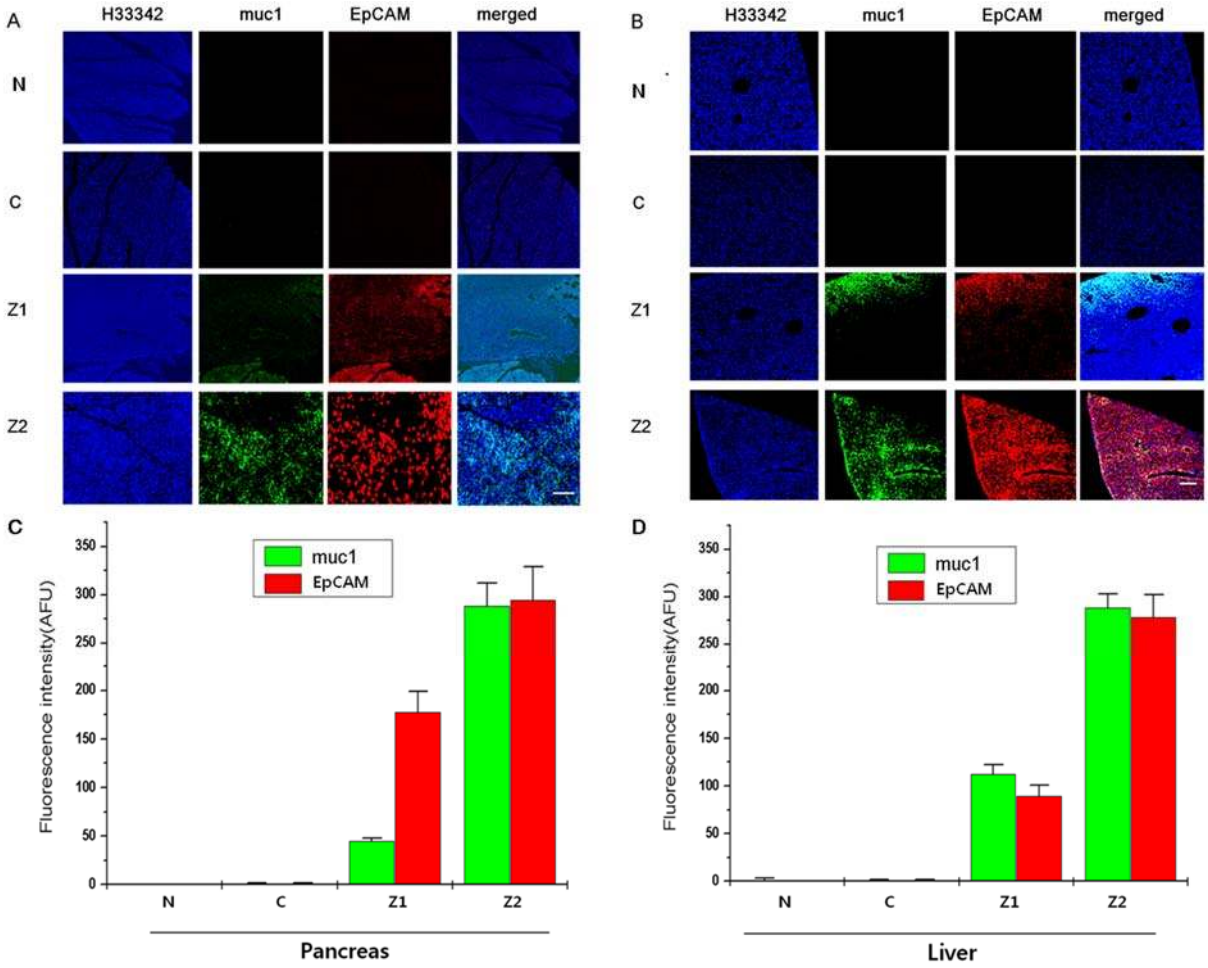

Figure 4.Confocal microscopic analysis for muc1 and EpCAM in the tissues.

Tissues were immunocytochemicaly stained to detect muc1 (green) and EpCAM (red) with H33342 (blue) to mark nuclei. Bars denote 55 μm. In the pancreas (A and C), both markers are strongly expressed in the Z2. However, these markers are weakly (in Z1 group) or rarely expressed (in N and C) in the other groups. Similar patterns are observed in the liver tissues (B and D).

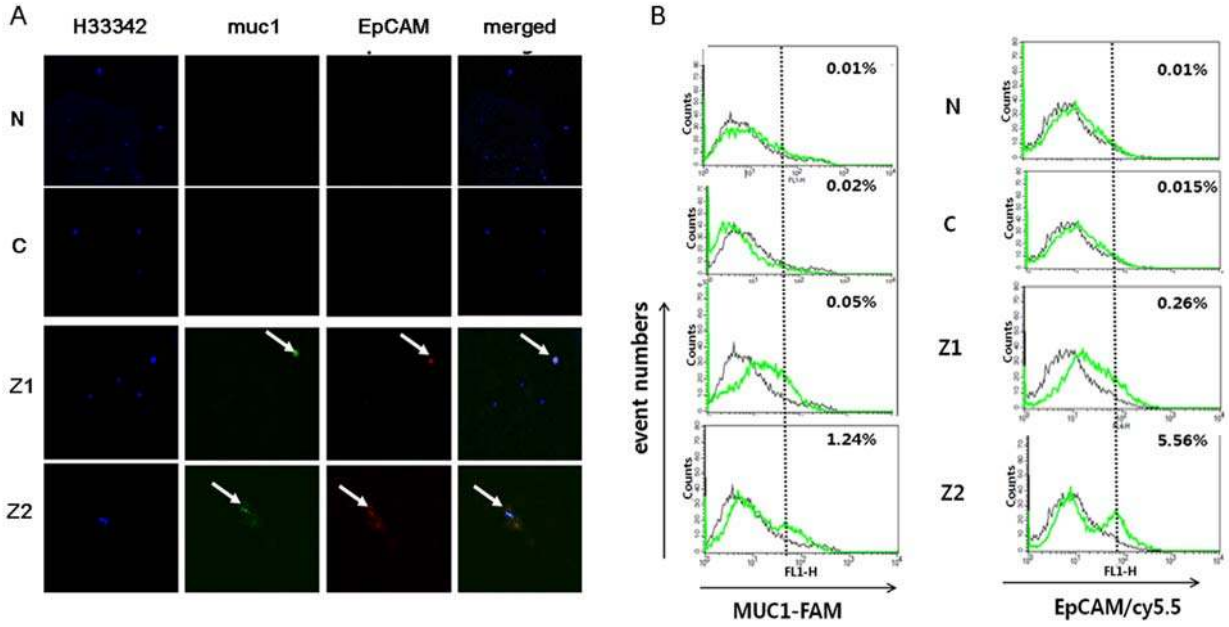

Figure 5. Muc1 and Ep-CAM expression in the mice blood

A. Confocal microscopy imaging of muc1(green) and EpCAM (red) by fluorescencing aptamer in mouse blood. EpCAM and muc1 were treated at room temperature and then cooled at 4 °C to initiate the hybridization.The nucleus was counterstained with H33342 (blue). In the N and C,no cells stained for Ep-CAM or muc1. In the Z2, larger circulating tumor cells (CTCs)-like cells stained for muc1 and EpCAM were observed, with sparse expression of muc1/EpCAM is shown in Z1. B. On FACScan, the expression of MUC1 and EpCAM was rarely seen in the N and C groups. In Z1, expression of MUC1 (0.05%) and EpCAM (0.26%) were slightly increased. In the Z-2 group, greater expression of MUC1 (1.24%) and EpCAM (5.56%) was noted.

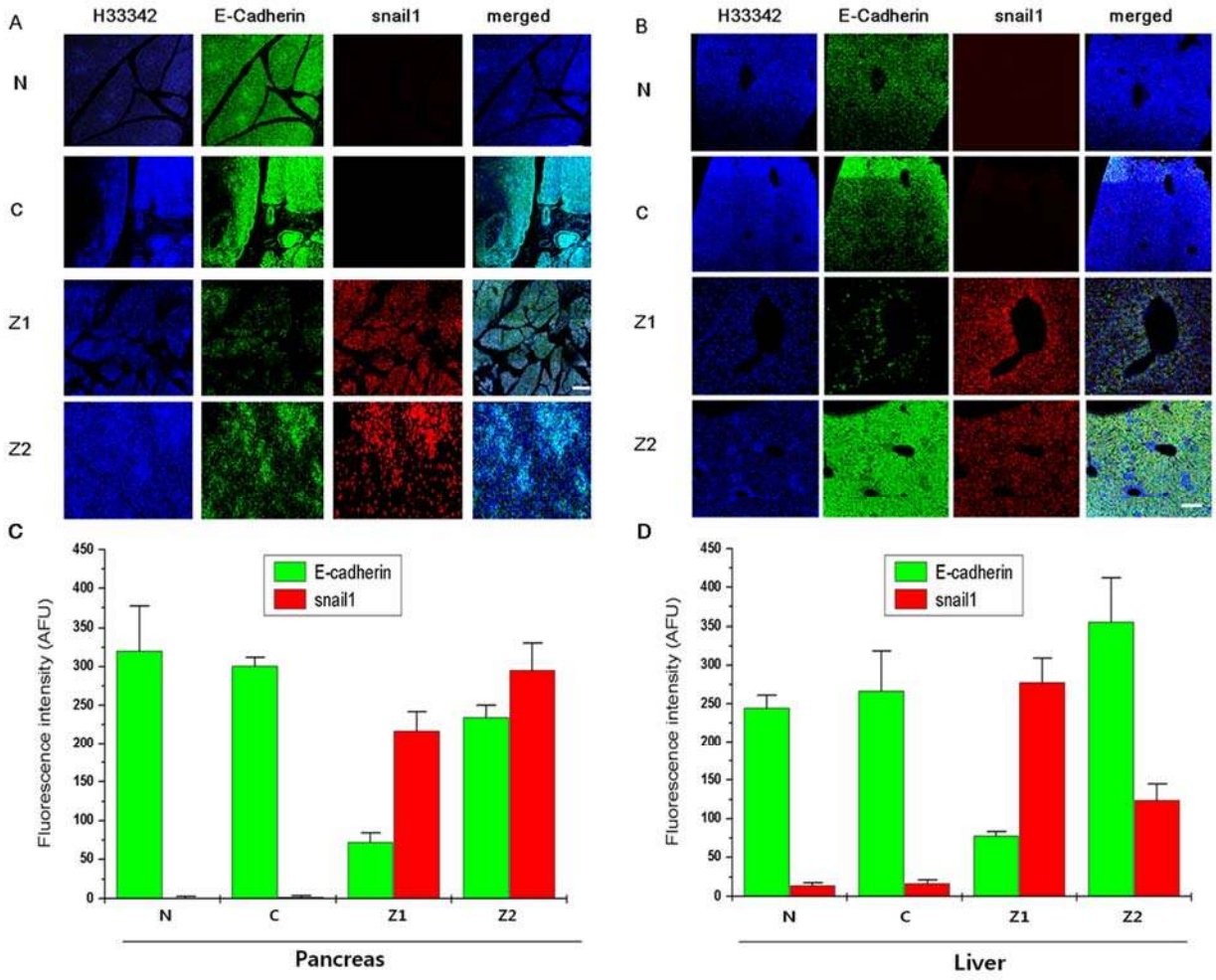

Figure 6.Confocal microscopytissue analysis of E-Cadherin and snail1.

Tissues were immunocytochemicaly stained to detect E-Cadherin (green) and snail1 (red) with H33342 (blue) to mark nuclei. Bars denote 55 μm. In the pancreas (A and C), prominent expression of Snail1 was observed in Z1, with greater expression in Z2, with no expression in N and C. E-Cadherin was strongly expressed in the N and C, and decreased in the Z1. In the liver (B and D), snail was expressed strongly in the Z1 and weakly in the Z2. However, weak expression was evident in the N and C groups. Expression of E-Cadherin was increased in the N, C and Z2 groups.

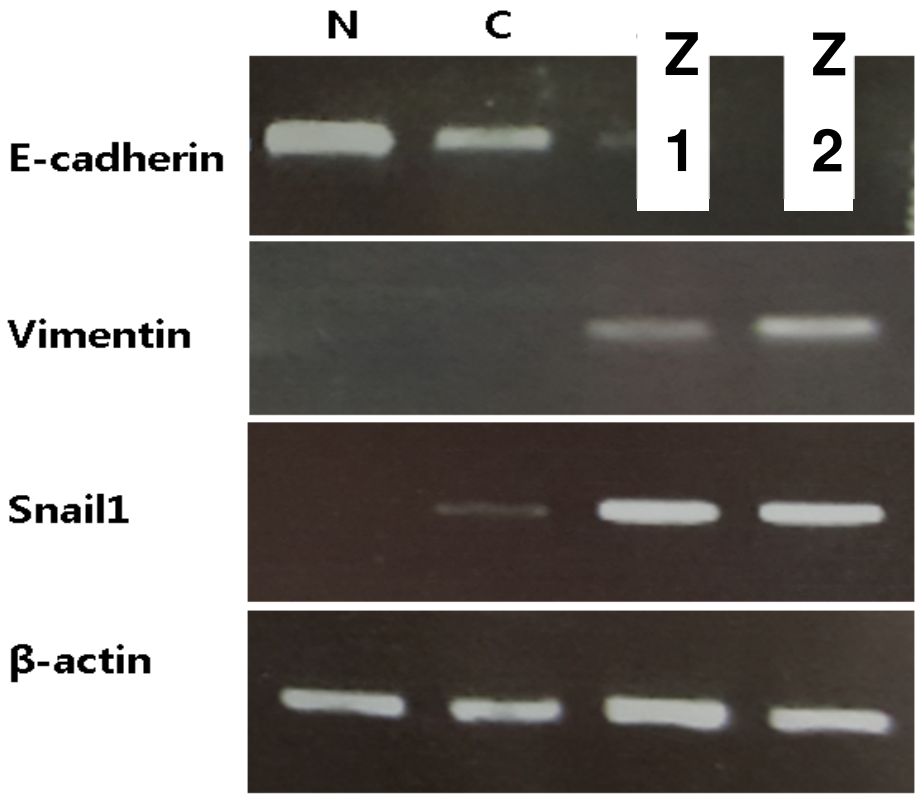

Figure 7.Evaluation E-cadherin, Vimentin and Snail1expression as EMT markers in the liver tissue by RT-PCR. The expression levels of vimentin and Snail1of the Z1 and Z2 were increased compared to N and C group. Furthermore, E-cadherin expression levels were significantly increased in N and C group compared to Z1 and Z2 groups. β–actin was used as housekeeping gene.

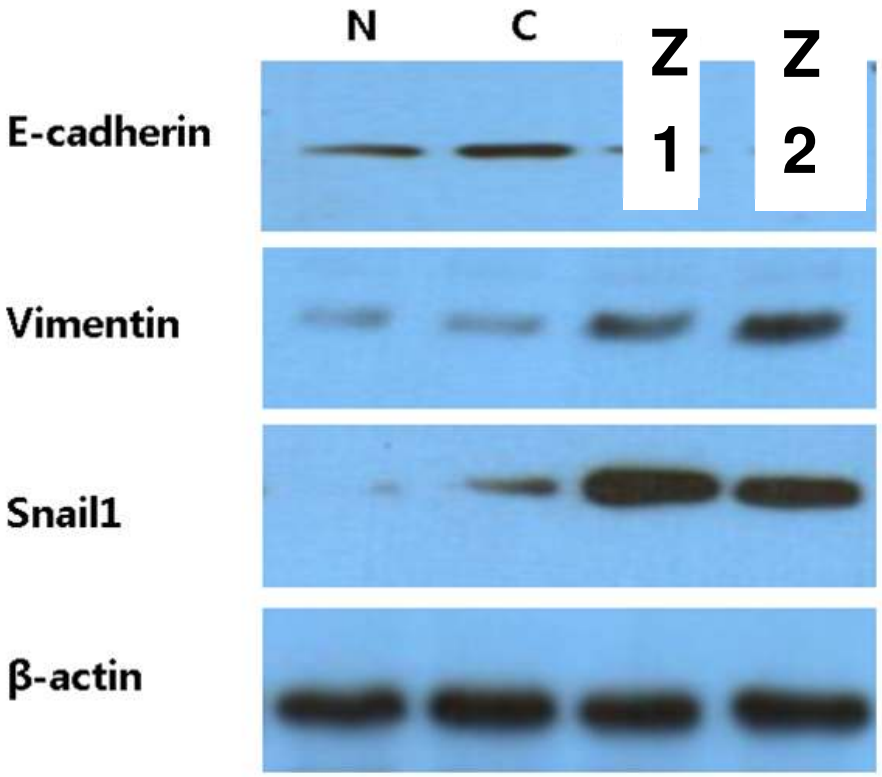

Figure 8. Evaluation E-cadherin, Vimentin and Snail1expression as EMT markers in the liver tissue by western blot analysis. Increased levels of Vimentin and Snail1and decreased level of E-Cadherin were observed in the Z and Z2 group compared to N and C group.

Discussion

Chronic inflammation leads host defenses and mediates tissue repair and regeneration, which may occur in infectious or non-infectious tissue damage. The long-standing inflammation due to chronic irritation can fuel development of dysplasia. Meanwhile, an inflammatory cytokine network may influence on gene alteration in tumor and stromal cells. In other ways, chronic inflammation that facilitates tumor progression creates local immune suppression.[24] Subsequently, these environments predispose to cancer.[24-26] Therefore, chronic inflammation can induce cancer development and contributes to the progression of cancer.[1-3] In contrast, acute inflammation does not cause chronic tissue irritation and may not induce cancer. However, when acute inflammation occurs in a cancer patient, the inflammation might contribute to cancer progression.

There are a few clinical conditions in which inflammation is directly caused by obstruction related to the tumor mass. In gallbladder cancer, as the cancer grows it may obstruct the cystic duct, which has a narrow diameter and is easily obstructed, resulting in acute cholecystitis. Bile duct cancer with cholangitis displays a similar mechanism. In both cancers, preoperative acute inflammation induced by cancer has a negative impact after surgical resection.[6, 7] These two cancers may offer optimal

clinical conditions for assessing the relationship between acute inflammation and cancer progression. In the present study, we designed a mouse model in which acute inflammation was induced after cancer formation, similar to the clinical setting.

It is still difficult to explain how acute inflammation is associated with a poor prognosis for cancer. However, it is widely accepted that the host inflammatory response, including cytokines and other chemical messengers, plays an important role in cancer growth and metastases. [3] Numerous molecules that play a critical role in inflammation have been identified, including tumor necrosis factor, interleukin-6, cyclooxygenase-2 and matrix metalloprotease. Many of them also play a critical role in cancer progression, not only in chronic inflammation, but also in acute inflammation..[26, 27]

Acute inflammation promotes EMT, which is expected to have a crucial role in cancer cell dissemination.[28] Activation of EMT promotes the early steps of metastasis, including local invasion, intravasation, extravasation and colonization. For cell proliferation and macrometastasis formation at distant sites, the loss of an EMT-inducing signal and reversion to an epithelial state (i.e., mesenchymal-epithelial transition, MET) are essential.[29,30] This EMT/MET process is critical in promoting metastasis in epithelium-derived carcinoma.[31] E-Cadherin is the most important mediator of cell-to-cell adhesion in the normal epithelial tissues. During MET,

repression of E-Cadherin occurs through E-Cadherin gene transcriptional repression, promoter methylation and protein degradation.[32-34] The loss of E-Cadherin is one of the definite features of EMT[35] and is related with poor prognosis in various cancer[36, 37]. Snail1 is the transcription factor directly binds to the E-Cadherin promoter and represses its transcription as well as transcription of Zeb1 and Twist1.[32] The expression of Vimentin is characteristic of epithelial cells undergoing the EMT process and it is related to reduced expression of E-Cadherin.[38] Therefore, during EMT, expression of Snail1 and Vimentin are increased and clinically, the expression of them in cancer cells is believed to enhance migration and metastasis.[14, 39] During the MET process, loss of EMT-inducing signal occurs by miR-200.[30] In the present study, strong expression of E-cadherin and rare expression of Snail1/ Vimentin were evident in the mice without inflammation (N and C groups; Figure 6-8). Thus, EMT did not occur in these mice. On the contrary, EMT was occurred in the Z1 and Z2 groups, Snail1 and Vimentin expression were increased in the pancreas and liver (Figure 6-8). On confocal analysis, the expression of E-Cadherin was relatively heterogeneous in the Z2 groups, repression of E-Cadherin did not occur in the Z2 group (Figure 6). However, decreased expression of E-Cadherin in Z1 and Z2 groups could be identified on RT-PCR and western blot (Figure 7-8). In many late state human carcinomas, E-Cadherin

expression appears to be heterogenous, with E-Cadherin-negative tumor cells interspersed within foci of E-Cadherin-positive areas in the tumor[40,41] This phenomenon means that the EMT/MET processes during metastasis are dynamic and occur simultaneously from the early to late stage of cancer.[31] Therefore, our results showed that acute inflammation facilitates EMT and MET.

In the present study, aptamers of EpCAM and muc1 were used to assess cancer progression. EpCAM is an epithelial cell adhesion molecule. It is a transmembrane glycoprotein expressed in the epithelium of healthy individuals, and which is over-expressed in most human adenocarcinomas.[42] Muc1, a transmembrane member of the mucin family, is expressed at a base level by normal ductal epithelial cells of secretary organs including the breast, lung and pancreas.[43] The occurrence of EpCAM positive disseminated tumor cells correlates with poor survival.[44] Similarly, elevated level of muc1 plays a role in human cancer progression, especially in the process of metastasis[43, 45] and is associated with shorter survival after surgical resection of cancer.[46, 47] Antibodies to EpCAM and muc1 are helpful for detection of CTCs in the blood.[16, 19]However, although patients with metastatic lesions are more likely to have CTCs detected in their blood, CTCs are rarely captured in the blood because of their lower numbers in blood and contamination by white blood cells.[19, 48]Moreover, false positive detection is common because of shared epitopes between

several proteins.[49] Aptamers, also known as chemical antibodies, are short single-stranded DNA or RNA isolated by systemic evolution of ligands by exponential enrichment (SELEX).[50] Aptamers can be chemically synthesized with minimal batch variation and are cost-effective. Moreover, they are capable of binding to target molecules with high affinity and selectivity.[51, 52] Because aptamers are 10 20 times smaller than an antibody, they have good tissue penetration ability and so can be more advantageous over antibodies in cancer targeting. In the present study, EpCAM and muc1 in blood could be detected using aptamers. In the Z2 group, expression of EpCAM and muc1 was observed in the blood, as well as in the pancreas and liver tissue. However, in the N and Z1 groups, these were not expressed in tissue or blood. EMT contributes to the intravasation of existed CTCs from the primary tumor site into the bloodstream, followed by transport to a secondary site where the cells extravasate, proliferate and form metastatic lesions.[19] In many cancers, the number of CTCs exhibiting EMT markers increases from the early to late stage.[18]Acute inflammation may induce EMT and facilitate intravasation and extravasation of CTCs from pancreas tumors to the area of metastasis.

In the present study, although metastatic liver nodules were found in only 50% of the Z2 group, most mice showed strong expression of EpCAM and muc1 in pancreatic and liver tissues. Moreover, expression of miR-155, which is a poor prognostic

factor in pancreatic cancer,[53] was also increased. However, expression of these biomarkers occurred rarely in the Z1 and C groups. Recent results in a mouse model showed that dissemination of tumor cells for metastasis from the pancreas can occur prior to tumor formation.[28] Markers for EMT and CTCs can be used as a predictor for metastases when a metastatic tumor was not formed yet.[28, 54] In the Z2 group, the environment of metastasis may have resulted from the acute inflammation; if mice had survived longer, clinical metastasis would be appeared in all mice. These results support the view that acute inflammation facilitates tumor progression and metastasis, and creates an environment conducive for the development of clinical metastasis.

Although the relationship between the degree of acute inflammation and cancer progression remains unknown, our study suggested possible correlation between degree of inflammation and cancer progression. Intraperitoneal injection of zymosan, a polysaccharide cell wall component derived from *Saccharomyces cerevisiae*and a glucan with repeating glucose units connected by β-1,3-glycosidic linkages, has been widely used in a self-resolving model of acute inflammation. By intraperitoneal injection, it induces moderate to severe acute local and systemic inflammation by leukocyte recruitment and releasing inflammatory cytokines, such as leukotrien B4, IL-1, IL-6 and TNF, and induces local and systemic inflammation.[55, 56]This inflammatory reaction is similar to the clinical setting. However, inflammation induced

by zymosan resolves within 2–3 days and this short acting acute inflammation would not affect cancer progression. Therefore, sustainable inflammation may be needed to magnify the impact of acute inflammation, and zymosan was injected repeatedly in the Z2 group. The second injection of zymosan resulted in marked increase in level of cytokines and influx of neutrophils, consistent with the compound' s ability to induce effective sustainable and strong inflammation.[57] In the Z2 group, infiltration of inflammatory cell in the pancreas was more frequent in histopathological examination. Moreover, colocalization of inflammatory marker, NLRP3 for inflammasome formation[58, 59] was significantly stronger than those of the C and Z1 groups. Inflammasomes are a group of cytosolic protein complexes that participate in the secretion of IL-1β and IL-18. The inflammasome is activated by expression of NLRP3 and is assembled after exposure to microbial toxins. NLRP3 mediated activation of the inflammasome can lead to excessive inflammatory responses. miR-155, which is a poor prognostic factor of pancreatic cancer,[53] has an immune regulatory function. It regulates inflammatory cytokines, macrophages, and activation of T-cells and B-cells.[59] Therefore, expression of miR-155 in our study might have indicated the effective creation of inflammation as well as creation of a poor environment of cancer progression by inflammation. The expression of NLRP3 and miR-155 in the tissues were increased in proportion to the injection dose of zymosan,

with rare expression in the N and C groups, moderate expression in the Z1 group and markedly elevated expression in the Z2 group (Figure 3). These observations suggest that repeated injection of zymosan could effectively induce acute inflammation. Tumor progression in the Z1 group was not different compared to the control group, while tumor volume was bigger and liver metastasis was more frequent in the Z2 group compared to the C group. Furthermore, occurrence of EMT and detection of CTCs were significantly prominent in the Z2 group, while they were not in the C and Z1 groups. Thus, if inflammation is not strong and is temporary, the effect of acute inflammation on cancer progression would be minimized. Therefore, acute and sustainable strong inflammation may affect aggressive tumor progression.

Although there are a few clinical studies of negative outcome of local and systemic inflammatory responses in gallbladder cancer, cholangiocarcinoma, colon cancer and pancreas cancer[6, 7, 60, 61] there are still controversies for impact of inflammation on cancer, even positive effect of inflammation on colorectal cancer[62]. Moreover, the basic pathophysiology for a poor prognosis related to acute inflammation is still elusive. This preclinical experimental study showed that acute inflammation facilitates cancer progression and distant metastasis. Further studies with western blot or RT-PCR are necessary to validate our results. If this molecular mechanism is revealed, target therapy against acute inflammation can be useful for improving the

long term prognosis after surgical resection of the cancer.

In conclusion, acute inflammation accompanied with cancer promotes cancer progression and metastasis.

Reference

1. Garcea G, Dennison AR, Steward WP, et al. Role of inflammation in pancreatic carcinogenesis and the implications for future therapy. Pancreatology 2005; 5:514-29.
2. Ernst PB, Gold BD. The disease spectrum of Helicobacter pylori: the immunopathogenesis of gastroduodenal ulcer and gastric cancer. Annu Rev Microbiol 2000; 54:615-40.
3. Coussens LM, Werb Z. Inflammation and cancer. Nature 2002; 420:860-7.
4. Balkwill F, Mantovani A. Inflammation and cancer: back to Virchow? Lancet 2001; 357:539-45.
5. Mantovani A, Allavena P, Sica A, et al. Cancer-related inflammation. Nature 2008; 454:436-44.
6. Cho JY, Han HS, Yoon YS, et al. Preoperative cholangitis and metastatic lymph node have a negative impact on survival after resection of extrahepatic bile duct cancer. World J Surg 2012; 36:1842-7.
7. Han HS, Cho JY, Yoon YS, et al. Preoperative inflammation is a prognostic factor for gallbladder carcinoma. Br J Surg 2011; 98:111-6.
8. Crozier JE, McKee RF, McArdle CS, et al. Preoperative but not postoperative systemic inflammatory response correlates with survival in colorectal cancer.

Br J Surg 2007; 94:1028-32.

9. van der Gaag NA, Harmsen K, Eshuis WJ, et al. Pancreatoduodenectomy associated complications influence cancer recurrence and time interval to death. Eur J Surg Oncol 2014; 40:551-8.

10. Cho JY, Han HS, Yoon YS, et al. Postoperative complications influence prognosis and recurrence patterns in periampullary cancer. World J Surg 2013; 37:2234-41.

11. Law WL, Choi HK, Lee YM, et al. The impact of postoperative complications on long-term outcomes following curative resection for colorectal cancer. Ann Surg Oncol 2007; 14:2559-66.

12. Yang J, Weinberg RA. Epithelial-mesenchymal transition: at the crossroads of development and tumor metastasis. Dev Cell 2008; 14:818-29.

13. Chaffer CL, Thompson EW, Williams ED. Mesenchymal to epithelial transition in development and disease. Cells Tissues Organs 2007; 185:7-19.

14. Wu Y, Deng J, Rychahou PG, et al. Stabilization of snail by NF-kappaB is required for inflammation-induced cell migration and invasion. Cancer Cell 2009; 15:416-28.

15. Li CW, Xia W, Huo L, et al. Epithelial-mesenchymal transition induced by TNF-alpha requires NF-kappaB-mediated transcriptional upregulation of

Twist1. Cancer Res 2012; 72:1290-300.

16. Yu M, Stott S, Toner M, et al. Circulating tumor cells: approaches to isolation and characterization. J Cell Biol 2011; 192:373-82.

17. Yu M, Bardia A, Wittner BS, et al. Circulating breast tumor cells exhibit dynamic changes in epithelial and mesenchymal composition. Science 2013; 339:580-4.

18. Kallergi G, Papadaki MA, Politaki E, et al. Epithelial to mesenchymal transition markers expressed in circulating tumour cells of early and metastatic breast cancer patients. Breast Cancer Res 2011; 13:R59.

19. Maheswaran S, Haber DA. Circulating tumor cells: a window into cancer biology and metastasis. Curr Opin Genet Dev 2010; 20:96-9.

20. Komoto M, Nakata B, Nishii T, et al. In vitro and in vivo evidence that a combination of lapatinib plus S-1 is a promising treatment for pancreatic cancer. Cancer Sci 2010; 101:468-73.

21. Jonckheere N, Fauquette V, Stechly L, et al. Tumour growth and resistance to gemcitabine of pancreatic cancer cells are decreased by AP-2alpha overexpression. Br J Cancer 2009; 101:637-44.

22. Song Y, Zhu Z, An Y, et al. Selection of DNA aptamers against epithelial cell adhesion molecule for cancer cell imaging and circulating tumor cell capture.

Anal Chem 2013; 85:4141-9.

23. Subramanian N, Kanwar JR, Athalya PK, et al. EpCAM aptamer mediated cancer cell specific delivery of EpCAM siRNA using polymeric nanocomplex. J Biomed Sci 2015; 22:4.

24. Muller AJ, Sharma MD, Chandler PR, et al. Chronic inflammation that facilitates tumor progression creates local immune suppression by inducing indoleamine 2,3 dioxygenase. Proc Natl Acad Sci U S A 2008; 105:17073-8.

25. Kamp DW, Shacter E, Weitzman SA. Chronic inflammation and cancer: the role of the mitochondria. Oncology (Williston Park) 2011; 25:400-10, 13.

26. Allavena P, Garlanda C, Borrello MG, et al. Pathways connecting inflammation and cancer. Curr Opin Genet Dev 2008; 18:3-10.

27. Halin C, Detmar M. Chapter 1. Inflammation, angiogenesis, and lymphangiogenesis. Methods Enzymol 2008; 445:1-25.

28. Rhim AD, Mirek ET, Aiello NM, et al. EMT and dissemination precede pancreatic tumor formation. Cell 2012; 148:349-61.

29. Boyer B, Thiery JP. Epithelium-mesenchyme interconversion as example of epithelial plasticity. Apmis 1993; 101:257-68.

30. Tsai JH, Donaher JL, Murphy DA, et al. Spatiotemporal regulation of epithelial-mesenchymal transition is essential for squamous cell carcinoma

metastasis. Cancer Cell 2012; 22:725-36.

31. Tsai JH, Yang J. Epithelial-mesenchymal plasticity in carcinoma metastasis. Genes Dev 2013; 27:2192-206.

32. Batlle E, Sancho E, Franci C, et al. The transcription factor snail is a repressor of E-cadherin gene expression in epithelial tumour cells. Nat Cell Biol 2000; 2:84-9.

33. Saito Y, Takazawa H, Uzawa K, et al. Reduced expression of E-cadherin in oral squamous cell carcinoma: relationship with DNA methylation of 5' CpG island. Int J Oncol 1998; 12:293-8.

34. Lester RD, Jo M, Montel V, et al. uPAR induces epithelial-mesenchymal transition in hypoxic breast cancer cells. J Cell Biol 2007; 178:425-36.

35. Hazan RB, Qiao R, Keren R, et al. Cadherin switch in tumor progression. Ann N Y Acad Sci 2004; 1014:155-63.

36. Lazar D, Taban S, Ardeleanu C, et al. The immunohistochemical expression of E-cadherin in gastric cancer; correlations with clinicopathological factors and patients' survival. Rom J Morphol Embryol 2008; 49:459-67.

37. Breyer J, Gierth M, Shalekenov S, et al. Epithelial-mesenchymal transformation markers E-cadherin and survivin predict progression of stage pTa urothelial bladder carcinoma. World J Urol 2015.

38. Zhao Y, Yan Q, Long X, et al. Vimentin affects the mobility and invasiveness of prostate cancer cells. Cell Biochem Funct 2008; 26:571-7.

39. Yang CC, Wolf DA. Inflamed snail speeds metastasis. Cancer Cell 2009; 15:355-7.

40. Bukholm IK, Nesland JM, Karesen R, et al. E-cadherin and alpha-, beta-, and gamma-catenin protein expression in relation to metastasis in human breast carcinoma. J Pathol 1998; 185:262-6.

41. Bonnomet A, Syne L, Brysse A, et al. A dynamic in vivo model of epithelial-to-mesenchymal transitions in circulating tumor cells and metastases of breast cancer. Oncogene 2012; 31:3741-53.

42. Baeuerle PA, Gires O. EpCAM (CD326) finding its role in cancer. Br J Cancer 2007; 96:417-23.

43. Kufe DW. Mucins in cancer: function, prognosis and therapy. Nat Rev Cancer 2009; 9:874-85.

44. Rao CG, Chianese D, Doyle GV, et al. Expression of epithelial cell adhesion molecule in carcinoma cells present in blood and primary and metastatic tumors. Int J Oncol 2005; 27:49-57.

45. Hollingsworth MA, Swanson BJ. Mucins in cancer: protection and control of the cell surface. Nat Rev Cancer 2004; 4:45-60.

46. Nagai S, Takenaka K, Sonobe M, et al. A novel classification of MUC1 expression is correlated with tumor differentiation and postoperative prognosis in non-small cell lung cancer. J Thorac Oncol 2006; 1:46-51.

47. Tsutsumida H, Goto M, Kitajima S, et al. Combined status of MUC1 mucin and surfactant apoprotein A expression can predict the outcome of patients with small-size lung adenocarcinoma. Histopathology 2004; 44:147-55.

48. Allard WJ, Matera J, Miller MC, et al. Tumor cells circulate in the peripheral blood of all major carcinomas but not in healthy subjects or patients with nonmalignant diseases. Clin Cancer Res 2004; 10:6897-904.

49. Bordeaux J, Welsh A, Agarwal S, et al. Antibody validation. Biotechniques 2010; 48:197-209.

50. Tuerk C, Gold L. Systematic evolution of ligands by exponential enrichment: RNA ligands to bacteriophage T4 DNA polymerase. Science 1990; 249:505-10.

51. Famulok M, Hartig JS, Mayer G. Functional aptamers and aptazymes in biotechnology, diagnostics, and therapy. Chem Rev 2007; 107:3715-43.

52. Pu Y, Zhu Z, Liu H, et al. Using aptamers to visualize and capture cancer cells. Anal Bioanal Chem 2010; 397:3225-33.

53. Greither T, Grochola LF, Udelnow A, et al. Elevated expression of microRNAs

155, 203, 210 and 222 in pancreatic tumors is associated with poorer survival. Int J Cancer 2010; 126:73-80.

54. Thege FI, Lannin TB, Saha TN, et al. Microfluidic immunocapture of circulating pancreatic cells using parallel EpCAM and MUC1 capture: characterization, optimization and downstream analysis. Lab Chip 2014; 14:1775-84.

55. Goris RJ, Boekholtz WK, van Bebber IP, et al. Multiple-organ failure and sepsis without bacteria. An experimental model. Arch Surg 1986; 121:897-901.

56. Mahesh J, Daly J, Cheadle WG, et al. Elucidation of the early events contributing to zymosan-induced multiple organ dysfunction syndrome using MIP-1alpha, C3 knockout, and C5-deficient mice. Shock 1999; 12:340-9.

57. Rao TS, Currie JL, Shaffer AF, et al. In vivo characterization of zymosan-induced mouse peritoneal inflammation. J Pharmacol Exp Ther 1994; 269:917-25.

58. Kim JJ, Jo EK. NLRP3 inflammasome and host protection against bacterial infection. J Korean Med Sci 2013; 28:1415-23.

59. Mashima R. Physiological roles of miR-155. Immunology 2015; 145:323-33.

60. McMillan DC, Canna K, McArdle CS. Systemic inflammatory response predicts survival following curative resection of colorectal cancer. Br J Surg 2003;

90:215-9.

61. Pine JK, Fusai KG, Young R, et al. Serum C-reactive protein concentration and the prognosis of ductal adenocarcinoma of the head of pancreas. Eur J Surg Oncol 2009; 35:605-10.

62. Roxburgh CS, Salmond JM, Horgan PG, et al. The relationship between the local and systemic inflammatory responses and survival in patients undergoing curative surgery for colon and rectal cancers. J Gastrointest Surg 2009; 13:2011-8.

국문 초록

실험 동물 모델에서 자이모산을 이용한 급성 염증이 췌장암의 성장과 전이에 미치는 영향에 대한 연구

안근수

의학과 외과학 전공

서울대학교 대학원

연구배경 임상적으로 급성 염증이 종양의 성장에 영향을 미칠 것으로 생각되고 있지만 여기에 대해 아직 전임상 및 임상 연구 결과가 보고된 경우는 드물다. 본 연구에서 실험쥐를 이용하여 복강내 급성 염증이 암의 성장에 미치는 영향을 연구하고자 한다.

연구재료 및 방법 실험쥐(C57/BL6) 에서 암을 유발하기 위하여 쥐 유래 췌장암 암세포주 (Panc-02)를 사용하였고 복강내 급성 염증을 유발하기 위해 자이모산을 복강내 주입하였다. 대조군 (n=10. C군)에서는 Panc-02 세포주 $2x10^7$ 개를 췌장 미부에 주입 후 4주 후 부검을 시행하였다. 제1실험군 (n=10, Z1군)은 세포주 주입 1주 후 3mg의 자이모산을 복강 내에 주입하였고 세포주 주입 4주 후 부검하였다. 제2실험군 (n=10, Z2군)은 세포주 주입 1,3주 후 두번에 걸쳐 각각 3mg의 자이모산을 복강 내 주입하였

고, 세포주 주입 4주 후 부검하였다. 종양의 형성 및 성장과 염증의 정도를 확인하기 위하여 병리조직 검사를 시행하였고 동일초점 현미경, 역전사-중합효소 연쇄 반응, 웨스턴 블롯 분석을 이용하여 췌장 및 간조직에서 EpCAM, muc1, E-Cadherin, Snail1, NLRP3, miR-155, Vimentin의 발현을 분석하였다. 또한 동일초점 현미경과 유세포 분석기를 이용하여 혈액 내 EpCAM과 muc1의 발현을 분석하였다.

결과 30마리의 실험쥐 중 부검 전 사망한 4마리와 종양이 형성 되지 않은 3마리를 제외한 23마리를 부검 하였다. 병리 조직 검사상 Z2 군에서 C 군에 비교하여 유의한 종양 크기의 증가 (P=0.021)와 간전이의 빈도(P=0.025)를 보였다. Z2군에서 다른 군에 비해 유의하게 심한 염증세포의 침윤이 보였다. 동일초점 현미경 분석 상 Z2 군에서 간과 췌장 모두에서 EpCAM, muc1, NLRP3, miR-155의 발현이 다른 군들에 비해 유의하게 증가 되었다. 동일초점 현미경과 유세포 분석기 검사 상 Z2군에서 혈액내 EpCAM과 muc1 발현이 다른 군들에 비해 유의하게 증가하였다. 역전사-중합효소 연쇄 반응과 웨스턴 블롯 분석 상 Z1과 Z2 군에서 Sanil1, Vimentin의 발현이 C군에 비해 유의하게 증가되었고 반대로 E-Cadherin은 Z1과 Z2군에서 발현이 유의하게 억제되었다.

결론 급성 염증은 상피간엽이행 (Epithelial-mesenchymal transition)을 통한 혈중 암세포(circulating tumor cell)가 증가되는 과정을 통하여 암의 성장과 전이를 촉진시킨다.

중심단어 : 급성 염증, 암, 상피간엽이행, 혈중 암세포

학 번 : 2011-31125